RESEARCH LETTER

Midostaurin as the Most Likely Cause of Bilateral Adrenal Masses in a Patient with Acute Myeloid Leukemia

Tim Schutte[1] · Claudia A. M. Stege[2] · Mark M. Smits[3] · Laurens E. Franssen[2] · Marjolein L. Donker[2] · David C. de Leeuw[2]

Midostaurin is an FMS-related tyrosine kinase 3 (FLT3) inhibitor commonly used for the treatment of FLT3 mutated acute myeloid leukemia (AML). This therapy is generally well tolerated, with known side effects including neutropenia, nausea, and headaches. Here, we describe the first human case of a probable new adverse drug reaction (ADR) with midostaurin in a patient with AML.

Case: A 77-year-old male presented to the emergency department with febrile neutropenia and headache. His relevant medical history included recently diagnosed FLT3-internal tandem duplication (ITD) AML (see the electronic supplementary material for medical history and co-medication). Initial cytoreductive treatment with hydroxyurea was started because of hyperleukocytosis (137×10^9/L) and skin chloroma (extra medullary 'solid' manifestation of AML). The patient was counseled for further treatment options and

✉ Tim Schutte
    t.schutte@amsterdamumc.nl

    Claudia A. M. Stege
    c.stege@amsterdamumc.nl

    Mark M. Smits
    mm.smits1@amsterdamumc.nl

    Laurens E. Franssen
    l.franssen@amsterdamumc.nl

    Marjolein L. Donker
    m.donker@amsterdamumc.nl

    David C. de Leeuw
    d.deleeuw@amsterdamumc.nl

1   Department of Medical Oncology, Amsterdam UMC
    Location Vrije Universiteit Amsterdam, Boelelaan 1117,
    Amsterdam, The Netherlands

2   Department of Hematology, Amsterdam UMC Location
    Vrije Universiteit Amsterdam, Boelelaan 1117, Amsterdam,
    The Netherlands

3   Department of Endocrinology, Amsterdam UMC Location
    Vrije Universiteit Amsterdam, Boelelaan 1117, Amsterdam,
    The Netherlands

deemed ineligible for intensive chemotherapy because of his age combined with an increased hematopoietic stem cell transplantation–comorbidity index (HCT-CI) score due to polymyalgia rheumatica and angina pectoris. At the time, standard treatment in The Netherlands for these patients was monotherapy with a hypomethylating agent (decitabine or azacitidine) as venetoclax was not yet registered. Additionally, he was counseled for participation in the HOVON-155 study, a randomized, phase 2 study to assess the tolerability and efficacy of adding midostaurin to decitabine in older, unfit, AML, and high-risk myelodysplasia patients [1]. He chose to participate in this study and was randomized to receive additional midostaurin next to decitabine. The HOVON-155 schedule encompasses cycles of 28 days, the first 5–10 days decitabine, directly followed by daily midostaurin until 2 days before the following cycle [1].

After three cycles, he achieved a minimal residual disease (MRD) negative complete remission (CR) in bone marrow and his skin chloroma regressed. Because he developed headaches from the end of the third cycle, accompanied by febrile neutropenia, he was admitted to the hospital. Midostaurin was (temporarily) discontinued because of a suspect time association between the headaches and initiation of midostaurin, headaches being a frequently reported side effect [2]. Moreover, the febrile neutropenia was empirically treated, and diagnostic workup was performed including a computed tomography (CT) chest scan, mini-bronchoalveolar lavage (mini-BAL), and lumbar puncture. This lumbar puncture revealed no significant abnormalities; however, two significant results were identified (see Table 1 for detailed results). First of all, the mini-BAL was positive for Epstein–Barr virus (EBV), triggering us to determine serum EBV load, which was remarkably elevated (> 100,000 IU/mL) due to EBV reactivation (positive EBV viral capsid antigen IgG (VCA-IgG) and Epstein-Barr nuclear antigen IgG (EBNA-IgG)). Secondly, a CT chest showed the incidental finding of bilateral adrenal masses, new compared to

Table 1 Timeline of cycles and midostaurin exposure with results of abdominal imaging and endocrinology and hormonal assessment of adrenal mass

Chronological timeline

Time (days)	Cycle	Diagnostics
0	Initial presentation, start hydroxyurea	
15	screening for HOVON-155 study	
24	Cycle 1, day 1, start decitabine	
29		Chest CT (indication: coughing and mild fever): No adrenal masses
34	Cycle 1, day 11, start midostaurin	
53	Cycle 1, day 30, stop midostaurin	
55	Cycle 2, day 1, start decitabine	
65	Cycle 2, day 11, (re)start midostaurin	
92	Cycle 2, day 38, Stop midostaurin	
98	Cycle 3 (delayed), day 1, start decitabine	
102	Cycle 3 premature end of decitabine (4 of 5 days completed, because of fever with neutropenia)	
104	Cycle 3, day 7, start midostaurin	
120	Admission with febrile neutropenia and headache	Chest CT: New adrenal masses Mini-BAL[a] (EBV+) and lumbar puncture (no significant abnormalities)[b]
122	Cycle 3, day 25, stop midostaurin due to headache	
125		EBV plasma load > 100,000 copies/mL
127		Dedicated abdominal CT: Adrenal masses: *Left*: 40 mm × 24 mm; density without contrast 35 HU, after contrast fluid 61 HU, washout phase 55 HU, absolute washout 23%, relative washout 10%. *Right*: 36 mm × 24 mm; density without contrast 37 HU, after contrast fluid 70 HU, washout phase 57 HU, absolute washout 39%, relative washout 19%[c]
129		EBV plasma load 67,000 copies/mL
140		EBV plasma load 1500 copies/mL
148		Abdominal CT: regression of adrenal masses: *left*: 30 mm × 14 mm; *right*: 20 mm × 13 mm
149		EBV plasma load undetectable

Endocrinology and hormonal assessment of adrenal mass

	Reference value	Measured value
Cortisol[d]	< 50 nmol/L	118 nmol/L
3-Methoxythyramine (blood)	< 0.10 nmol/L	< 0.08 nmol/L
Aldosterone (blood)[e]	0.03–0.54 nmol/L	< 0.03 nmol/L
Cortisol (blood)	250–650 nmol/L	118 nmol/L
Metanephrine (blood)	< 0.45 nmol/L	0.08 nmol/L
Normetanephrine (blood)	< 1.05 nmol/L	1.04 nmol/L
Renin activity (blood)	0–7.5 ng/mL/h	3.9 ng/mL/h
Volume (24-h urine)	NA	2100 mL
Creatinine (24-h urine)	9.0–19.0 mmol/24 h	8.2 mmol/24 h
Metanephrine (24-h urine)	< 1.52 μmol/24 h	0.42 μmol/24 h
Normetanephrine (24-h urine)	< 2.96 μmol/24 h[h]	3.84 μmol/24 h
3-Methoxythyramine (24-h urine)	< 2.75 μmol/24 h	2.81 μmol/24 h
Free cortisol (24-h urine)[f]	20–135 nmol/24 h	13 nmol/24 h
Cortisol (saliva)[g]	< 5 nmol/L	1.2 nmol/L

CT computed tomography, *EBV* Epstein–Barr virus, *HU* Hounsfield units, *mini-BAL* mini-bronchoalveolar lavage, *NA* not applicable

[a]Mini-BAL, all other cultures and RNA/DNA PCR for other pathogens were negative results: e.g., *Chlamydophila pneumonia/psittaci*,

Table 1 (continued)

Legionella pneumophila, *Mycobacterium* genus and tuberculosis, *Mycoplasma pneumonia*, *Pneumocystis jiroveci*, adenovirus, bocavirus, coronavirus, Human metapneumovirus, Herpes simplex virus type 1/2, influenza A/B, parainfluenza 1–4, rhinovirus/enterovirus, Respiratory syncytial virus, varicella-zoster virus, and severe acute respiratory syndrome coronavirus 2 (2019)

[b]Lumbar puncture results: leucocyte count $3 \times 10e6/L$; erythrocyte count (liquor) $0 \times 10^6/L$; glucose (liquor) 4.8 mmol/L; protein (liquor) 266 mg/L; culture (liquor): no micro-organisms detectable; HSV type 1/2 DNA PCR (liquor) negative; varicella-zoster virus DNA PCR (liquor) negative

[c]Absolute washout: $[(HU_{portal\ venous\ phase}) - (HU_{delayed})]/[(HU_{portal\ venous\ phase}) - (HU_{non-enhanced})] \times 100$; relative washout: $[(HU_{portal\ venous\ phase}) - (HU_{delayed})]/(HU_{portal\ venous\ phase}) \times 100$

[d]Overnight dexamethasone suppression test, 1 mg dexamethasone 23.00 h the evening before, next day cortisol between 08.00 and 09.00. The result of the test is a not-completely suppressed (i.e., <50 nmol/L) level of cortisol. However, this level is below 138 nmol/L (>5 μg/dL); values >138 following dexamethasone suppression suggest autonomous cortisol secretion. Values between 50 and 138 suggest possible autonomous cortisol secretion, and additional biochemical tests to confirm and assess the degree of cortisol secretion should be considered. Therefore, according to our local protocol, follow-up tests including a midnight saliva cortisol and 24-h urinalysis were performed. Both were completely normal. All results were discussed in a multidisciplinary expert team meeting. They concluded that endogenous or autonomous cortisol secretion could be excluded

[e]The undetectable plasma aldosterone level (<0.03 nmol/L) is explained by the use of an angiotensin-II receptor blocker (valsartan). This reduces the aldosterone production in the adrenal glands and explains the suppressed aldosterone levels that could induce renin production. The use of an angiotensin-II receptor blocker is a (slight) limitation to the sensitivity of the aldosterone–renin ratio to exclude hyperaldosteronism (M. Conn), although the dose of angiotensin-II receptor blocker (valsartan) the patient used is low (40 mg)

[f]The 24-h free urinary cortisol level was low and could potentially suggest adrenal cortex deficiency. However, these relatively low cortisol values were not further analyzed in the absence of symptoms of Addison's disease

[g]Midnight cortisol in saliva

[h]Reference values for normetanephrine (24-h urine) are age and sex specific. Here, we provided the reference value for males 60–69 years of age, as no specific reference values for patients ≥70 years of age are available from our laboratory

a CT chest 3–4 months earlier, which had been performed for the evaluation of coughing and fever (see Fig. 1 for the evolution of the adrenal masses over time).

At this point, our differential diagnosis of the bilateral adrenal masses included chloroma (although less likely given the reduction in skin chloroma and MRD negative CR state), EBV-associated adrenal tumors such as lymphoma, adrenocorticotropic hormone (ACTH) dependent adrenal hypertrophy, functioning adrenal adenoma or carcinoma, or midostaurin-induced adrenal hypertrophy (previously observed in animal studies). A timely diagnosis was essential to rule out progressive disease and determine the eligibility of treatment continuation with midostaurin and decitabine.

To rule out adrenal adenoma, we performed a specific abdominal CT with contrast for washout. Here, the left adrenal gland had a size of 40 mm, with a density of 35 Hounsfield units (HU) before contrast, an absolute washout of 23%, and relative washout of 10%. The right gland had a size of 36 mm, a density of 37 HU before contrast, an absolute washout of 39%, and relative washout of 19%. These values argued against adrenal adenomas (for which we would expect an attenuation value of <10 HU on unenhanced CT and higher rates of absolute and relative washout [3]).

Concomitantly, adrenal function tests were performed. As initial screening test for hypercortisolism, the overnight dexamethasone suppression test revealed a (minimal) insufficiently suppressed cortisol (see Table 1, endocrinological evaluation). Follow-up included midnight saliva cortisol and 24-h urinalysis that excluded hypercortisolism. A pheochromocytoma and hyperaldosteronism were improbable given the normal 24-h urine collection of metanephrines/catecholamines and normal plasma metanephrines and aldosterone/renin, respectively. Therefore, a functional adrenal adenoma was less likely.

To establish a definitive diagnosis, an endoscopic ultrasound (EUS)-guided fine-needle aspiration (FNA) was performed. Cytology of the left adrenal mass showed no signs of chloroma (blasts), adrenal carcinoma, lymphoma, or granuloma.

One week after EUS-guided FNA, the patient developed chest pain, located on the left dorsolateral chest. Regular evaluation with electrocardiogram (ECG) was unremarkable. Given the recent biopsy, a new CT was performed. This scan excluded adrenal bleeding, pulmonary embolism, or other complications. A remarkable observation was that the bilateral adrenal masses were significantly reduced in size (see timeline, Table 1, Fig. 1 and Supplemental content Fig. 1).

Given the regression of the adrenal masses in the absence of anti-leukemic therapy together with the cytology results and endocrinological assessment, the only un-excluded diagnosis and thus most likely clinical diagnosis is midostaurin-induced bilateral adrenal masses. When using the ADR probability scale/Naranjo algorithm [4], this ADR would be assessed as a "probable" ADR (see Supplemental content Table 2).

Given the possible benefit of midostaurin in our patient with FLT3-ITD AML and the asymptomatic nature of the
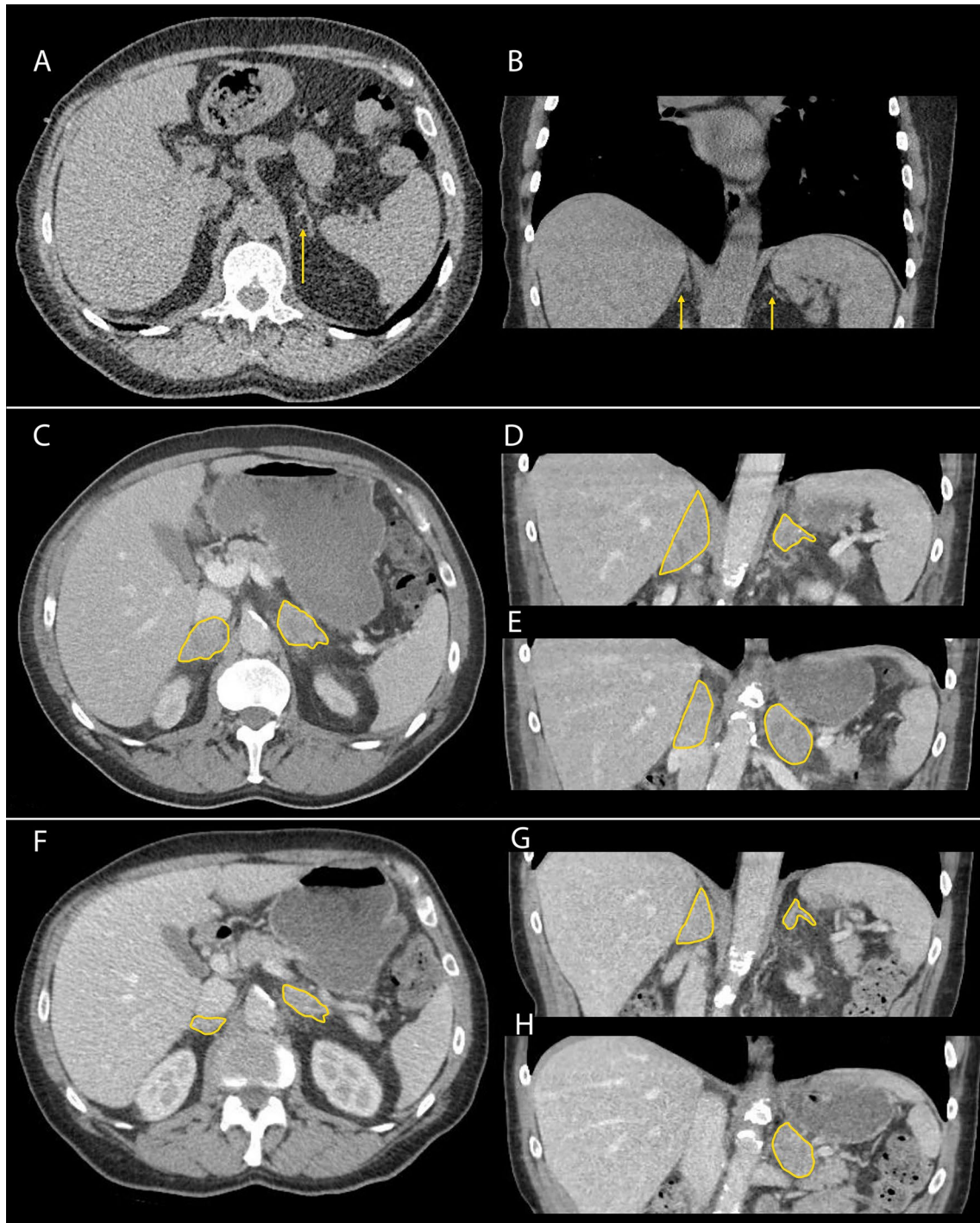
Fig. 1 CT images of the adrenal masses. Window **A** (transversal plane) and window **B** (coronal plane): day 29, no adrenal masses on CT chest. Window **C** (transversal plane) and windows **D** and **E** (coronal plane): day 127, dedicated abdominal CT with contrast medium washout; adrenal masses are indicated/outlined with a yellow line. Window **F** (transversal plane) and windows **G** and **H** (coronal plane): day 127, dedicated abdominal CT with contrast medium washout; adrenal masses are indicated/outlined with a yellow line and are regressing compared to day 127; for exact measurements, see Table 1. All CT images were aligned to show the largest adrenal diameters. Images at the 'same level' are sometimes difficult, as body positions differ. The images in our figure were selected/reviewed by a radiologist. *CT* computed tomography

incidental finding and regression of the adrenal masses, we re-initiated therapy. Unfortunately, no evaluations of the adrenal masses were performed thereafter, as this was not clinically indicated. The patient successfully continued therapy until AML relapse one and a half years after the initial diagnosis. He died shortly after due to a large intracerebral hemorrhage.

Midostaurin is a multi-targeted tyrosine kinase inhibitor (TKI) approved by the European Medicines Agency [2, 5] and US Food and Drug Administration (FDA) [6] for the treatment of patients with newly diagnosed FLT3 mutated AML combined with induction chemotherapy. This registration followed the promising results of the RATIFY trial, a phase 3 trial that evaluated addition of midostaurin to standard chemotherapy for AML with a FLT3 mutation [7]. In these patients, midostaurin prolonged overall and event-free survival [7]. Common side effects include neutropenia and headache, as also occurred in our patient. In addition to these known side effects, we report a first case of appearing and regressing adrenal masses following the initiation and discontinuation of midostaurin in men.

Although adrenal mass formation has not been described or reported in men so far [8], adrenal exposition to midostaurin and effects on adrenal biology have been reported in pre-clinical studies. The amount of [^{14}C]midostaurin in rats, 5 min after intravenous infusion, was 12–30 times higher in adrenal glands than in blood, as reported in the European Public Assessment Report (EPAR) [2]. Interestingly, not only adrenal disposition was substantial; cortical hypertrophy and dilated zona reticularis were also reported after exposition to midostaurin [2]. Likewise, an 18–31% increase in adrenal weight was observed in dogs at 26 weeks, with adrenal weight still being elevated at 12 months, reported in the FDA approval dossier of midostaurin [6]. This prolonged effect of adrenal weight in dogs at 12 months differs from our human case, given the regression of the masses following discontinuation. This is very rapid considering the extensive half-life of midostaurin and its active metabolites (up to 471 h) [2]. Moreover, the mechanism of how midostaurin influences adrenal biology or induces adrenal mass formation is still unclear [8]. The plausible role of midostaurin on adrenal biology further supported the presence of FLT3 receptors in cortical and medullary adrenal (canine) tissue [9]. Secondly, similar effects of high adrenal exposure and development of cortical hypertrophy and hyperplasia in rats, dogs, and monkeys were reported for quizartinib, a second-generation TKI developed for the treatment of FLT3 mutated AML [10].

Alternative causes that could have induced these bilateral adrenal masses are less likely based on our diagnostic findings; however, alternative etiology is inflammation caused by auto-immunopathies or infections. The most common adrenal infection is adrenal tuberculosis [11]. However, this is very unlikely, given the results of the FNA, which showed no signs of granulomas or necrosis, no suspect pulmonary lesions on previous chest imaging, and extensive diagnostics on the mini-BAL (day 120), which was negative for Auramine O staining, Tuberculosis culture, mycobacterium tuberculosis DNA Polymerase chain reaction (PCR), and *Mycobacterium* genus DNA PCR. Besides a mycobacterial infection, viral infections such as EBV and cytomegalovirus can cause adrenalitis, especially and almost exclusively in patients with primary or secondary immunodeficiency disorders [11]. Our patient experienced an EBV reactivation with an extremely high EBV load when his adrenal masses were identified. Moreover, due to his treatment, our patient had a secondary immunodeficiency disorder. However, we could not find cases in which adrenal masses were caused by an EBV infection, as a single diagnosis, without involvement of adrenal malignancy, chloroma, lymphoma, or metastasis. We did find reports of immunodeficient patients with adrenal masses and EBV (re)infections who presented with adrenal lymphoma, adrenal leiomyosarcoma, or smooth-muscle tumors [12–20]. In these cases, immunodeficiencies had a much longer duration (years compared to the very recent onset and short duration in our case), which combined with the FNA strongly argues against this etiology. In the course of our clinical workup, we considered this EBV reactivation and treatment with rituximab, but a spontaneous decline in EBV load from > 100,000 to 67,000 copies/mL within days and even further decrease to 1500 copies/mL the days thereafter let us decide to follow-up without treatment instead. Limitations of our report include choosing EUS-guided FNA (with a potential false negative rate for FNA of ± 10% for malignancy [21]) instead of biopsy, the latter also allowing the assessment of tissue histology and tests such as EBV PCR or EBV encoded RNA (EBER). However, we assessed percutaneous CT-guided histological biopsy as an intervention with higher complication risks. Furthermore, no ACTH was measured to formally exclude (ectopic) ACTH-secreting paraneoplastic syndrome and ACTH-driven adrenal hypertrophy. Although not measured directly, this etiology seems unlikely given that ACTH-dependent adrenal hypertrophy would likely induce elevated values of cortisol (which were normal). Moreover, such etiology is not likely to regress spontaneously. Finally, a follow-up CT scan of the adrenal masses after restart of midostaurin (rechallenge) would have been very useful to evaluate the probability of this ADR.

Patients treated with midostaurin are at risk of developing febrile neutropenia, for which CTs are regularly performed. Adrenal incidentalomas (or bilateral adrenal masses) can be found and require subsequent analysis. This report underlines the importance of including midostaurin-induced bilateral adrenal masses in the differential diagnosis and determining serum EBV load/serology in such cases. The definitive clinical diagnosis of midostaurin-induced bilateral adrenal masses

should only be diagnosed by exclusion of other causes. Given the possible benefit of the addition of midostaurin in our patient with FLT3-ITD AML and the asymptomatic nature of this incidental finding, we re-initiated therapy. The incidence, management, and long-term clinical relevance of FLT3 inhibitors, including midostaurin, and their relation with adrenal masses and potential role of EBV infection needs further study.

References

1. HOVON. https://hovon.nl/en/trials/ho155. Accessed 05 July 2022.
2. EMA. Assessment report of Midostaurin (Rydapt). https://www.ema.europa.eu/en/documents/assessment-report/rydapt-epar-public-assessment-report_en.pdf: European medicine agency—Committee for Medicinal Products for Human Use 2017. Accessed 05 July 2022.
3. Szolar DH, Korobkin M, Reittner P, Berghold A, Bauernhofer T, Trummer H, et al. Adrenocortical carcinomas and adrenal pheochromocytomas: mass and enhancement loss evaluation at delayed contrast-enhanced CT. Radiology. 2005;234(2):479–85.
4. Naranjo CA, Busto U, Sellers EM, Sandor P, Ruiz I, Roberts EA, et al. A method for estimating the probability of adverse drug reactions. Clin Pharmacol Ther. 1981;30(2):239–45.
5. Tzogani K, Yu Y, Meulendijks D, Herberts C, Hennik P, Verheijen R, et al. European Medicines Agency review of midostaurin (Rydapt) for the treatment of adult patients with acute myeloid leukaemia and systemic mastocytosis. ESMO Open. 2019;4(6): e000606.
6. FDA. Pharmacology and toxicology review and evaluation of Midostaurin (Rydapt). https://www.accessdata.fda.gov/drugsatfda_docs/nda/2017/207997Orig1Orig2s000PharmR.pdf: USA Food and drug administration - department of health and human services - center for drug evaluation and research; 2017. Accessed 07 July 2022.
7. Stone RM, Mandrekar SJ, Sanford BL, Laumann K, Geyer S, Bloomfield CD, et al. Midostaurin plus chemotherapy for acute myeloid leukemia with a FLT3 mutation. N Engl J Med. 2017;377(5):454–64.
8. Novartis. Personal communication from Novartis (the pharmaceutical company producing midostaurin) to D.C. de Leeuw: No previous reports of adrenal masses in patients treated with midostaurin. No additional information available of animal/pre-clinical studies on adrenal enlargement following midostaurin exposure; 2022.
9. Harding K, De Mello Souza CH, Shiomitsu K, Maxwell E, Bertran J. C-kit, flt-3, PDGFR-beta, and VEGFR2 expression in canine adrenal tumors and correlation with outcome following adrenalectomy. Can J Vet Res. 2021;85(4):279–84.
10. EMA. Assessment report of quizartinib (Vanflyta). https://www.ema.europa.eu/en/documents/assessment-report/vanflyta-epar-refusal-public-assessment-report_en.pdf: European medicine agency—Committee for Medicinal Products for Human Use 2019. Accessed 07 July 2022.
11. Upadhyay J, Sudhindra P, Abraham G, Trivedi N. Tuberculosis of the adrenal gland: a case report and review of the literature of infections of the adrenal gland. Int J Endocrinol. 2014;2014: 876037.
12. Barzon L, Trevisan M, Marino F, Guzzardo V, Palu G. Primary bilateral adrenal B-cell lymphoma associated with EBV and JCV infection. Infect Agent Cancer. 2009;4:1.
13. Ohkura Y, Shindoh J, Haruta S, Kaji D, Ota Y, Fujii T, et al. Primary adrenal lymphoma possibly associated with Epstein–Barr virus reactivation due to immunosuppression under methotrexate therapy. Medicine (Baltimore). 2015;94(31): e1270.
14. Ohsawa M, Tomita Y, Hashimoto M, Yasunaga Y, Kanno H, Aozasa K. Malignant lymphoma of the adrenal gland: its possible correlation with the Epstein–Barr virus. Mod Pathol. 1996;9(5):534–43.
15. Suankratay C, Shuangshoti S, Mutirangura A, Prasanthai V, Lerdlum S, Shuangshoti S, et al. Epstein–Barr virus infection-associated smooth-muscle tumors in patients with AIDS. Clin Infect Dis. 2005;40(10):1521–8.
16. Zetler PJ, Filipenko JD, Bilbey JH, Schmidt N. Primary adrenal leiomyosarcoma in a man with acquired immunodeficiency syndrome (AIDS). Further evidence for an increase in smooth muscle tumors related to Epstein–Barr infection in AIDS. Arch Pathol Lab Med. 1995;119(12):1164–7.
17. Sathe PA, Shah HU, Kothari KS, Ranganathan S, Kandalkar BM. Bilateral Epstein–Barr virus-associated adrenal leiomyomas in

a child without an established immunodeficiency. Pediatr Dev Pathol. 2012;15(4):329–32.

18. Brown DA, Deep NL, Driscoll CL, Link MJ, Jentoft ME, Daniels DJ. Synchronous Epstein–Barr virus-associated skull base and adrenal smooth-muscle tumors in an 8-year-old girl with recent Epstein–Barr virus infection. J Neurosurg Pediatr. 2018;22(3):283–7.

19. Petrilli G, Lorenzi L, Paracchini R, Ubiali A, Schumacher RF, Cabassa P, et al. Epstein–Barr virus-associated adrenal smooth muscle tumors and disseminated diffuse large B-cell lymphoma in a child with common variable immunodeficiency: a case report and review of the literature. Int J Surg Pathol. 2014;22(8):712–21.

20. Rashidi A, Fisher SI. Primary adrenal lymphoma: a systematic review. Ann Hematol. 2013;92(12):1583–93.

21. Martinez M, LeBlanc J, Al-Haddad M, Sherman S, DeWitt J. Role of endoscopic ultrasound fine-needle aspiration evaluating adrenal gland enlargement or mass. World J Nephrol. 2014;3(3):92–100.